# Nanoscale

Accepted Manuscript


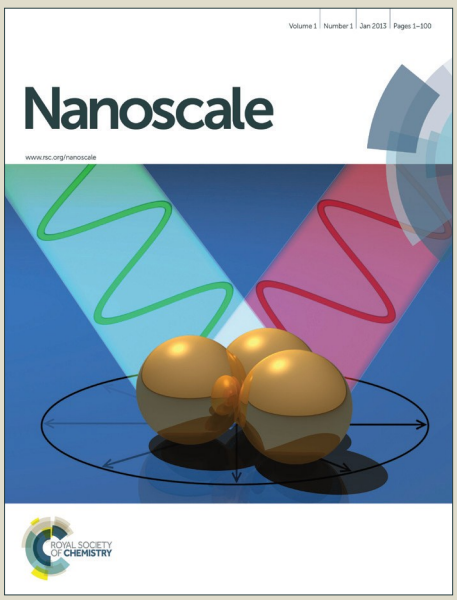





ROYAL SOCIETY OF CHEMISTRY

www.rsc.org/nanoscale

Journal Name

RSCPublishing

COMMUNICATION

# Colloidal $BiF_3$ nanocrystals: a bottom-up approach to conversion-type Li-ion cathodes

Cite this: DOI: 10.1039/x0xx00000x

Marek F. Oszajca,[a, b] Kostiantyn V. Kravchyk,[a, b] Marc Walter,[a, b] Franziska Krieg,[a, b] Maryna I. Bodnarchuk,[a, b] and Maksym V. Kovalenko[a, b]

Received 00th January 2012,
Accepted 00th January 2012

DOI: 10.1039/x0xx00000x

www.rsc.org/

**A facile colloidal synthesis of $BiF_3$ nanocrystals (NCs) via thermal decomposition of bismuth(III) trifluoroacetate in oleylamine is reported. The NC size can be tuned from 6 to 40 nm by the adjustment of synthesis parameters. After removal of the capping surfactant molecules, $BiF_3$ NCs were tested as a cathode material for Li-ion batteries. Close to theoretical Li-ion storage capacities of up to 300 mAh $g^{-1}$ at an average voltage of 3 V were obtained at current densities of 50 mA $g^{-1}$.**

Since its introduction in the 1990s, Li-ion battery technology has become the main source of energy in the majority of portable electronic devices. Further improvements of Li-ion batteries in terms of energy density and cycling stability are needed to meet the growing demands of such applications as electric vehicles and, in the near future, grid storage.[1] Nanostructured materials hold great promise as future high-energy-density cathode and anode materials. Colloidal NCs, owing to their well-defined size, shape and composition, and facile solution processing, are being actively pursued as novel electrode materials for Li-ion batteries, primarily in exploratory academic research[2-11] Downsizing of Li storage materials largely obviates common limitations such as poor electronic or ionic conductivity, slow reaction kinetics or large volumetric changes.[12] Downsizing also increasingly matters also for commercially viable materials. As an example, intercalation-type $LiFePO_4$ cathode has been commercialized only after its mean primary crystallite size was reduced to 100 nm and below.[13] Downsizing is even more critical for conversion- and alloying-type electrode materials. Colloidal NCs, synthesized via a purely bottom-up approach using molecular precursors, provide ideal model systems for understanding the effects of size, morphology and surface-chemistry on electrode performance.[5]

Despite the undisputable progress in nanostructured anodes based on alloying elements (silicon, tin, germanium and antimony, and their mixtures) and conversion-type compounds (oxides, sulfides),[14, 15] less attention has been dedicated to conversion-type cathode materials. The total theoretical charge storage capacity of a battery ($C_{total}$) can be calculated as $C_{total}=C_AC_C/(C_A+C_C)$, where $C_A$ and $C_B$ are the theoretical capacities of the cathode and anode, respectively. Without improving the capacity of the cathode-side of the battery, and replacing only the graphite anode with one of the aforementioned high-energy-density alternatives, $C_{total}$ can be improved by at most 21% for Sn, 25% for Ge and 32% for Si. In this work, we report the synthesis of high charge-storage capacity cathode material bismuth trifluoride, $BiF_3$, in the form of uniform colloidal NCs.

In conversion-type electrode materials, the bulk of the active material undergoes the following general electrochemical reaction:

$$M_aX_b + (b{\cdot}n)\ Li \leftrightarrow a\ M + b\ Li_nX$$

Here, M is the metal, X is theanion and n is the formal oxidation state of X.[16] $BiF_3$ is a highly promising cathode material due to its conversion to $Bi^0$ + 3 LiF via a three-electron reduction reaction (during discharge), occurring at an average voltage of ~3 V. Due to high specific weight of Bi, the theoretical specific capacity of $BiF_3$ is very high (302 mAh $g^{-1}$), corresponding to an energy density of ~900 Wh $kg^{-1}$, almost two times higher than that of commercial $LiFePO_4$ (one-electron reduction, 169 mAh $g^{-1}$, ~3.5 V and 590 Wh $kg^{-1}$) and $LiCoO_2$ (half-electron reduction, 135 mAh $g^{-1}$, ~3.9 V and 560 Wh $kg^{-1}$). Due to the high density of Bi (8.83 g $cm^{-3}$), its volumetric capacity is 2666 mAh $cm^{-3}$ (8000 Wh $L^{-1}$), almost three times that of $LiFePO_4$ and $LiCoO_2$. Wide-bandgap $BiF_3$ is an electrical insulator and cannot be used as an electrode material in bulk form. Top-down size reduction by high energy ball milling has been, so far, the main pathway to obtain nanostructured $BiF_3$; the resulting materials exhibit near-theoretical Li storage capacities.[17-22] The first example of bottom-up synthesized $BiF_3$ NCs was recently reported,[23] however, with the large crystallite size of these NCs of >100 nm and the lack of investigation of their Li storage properties.

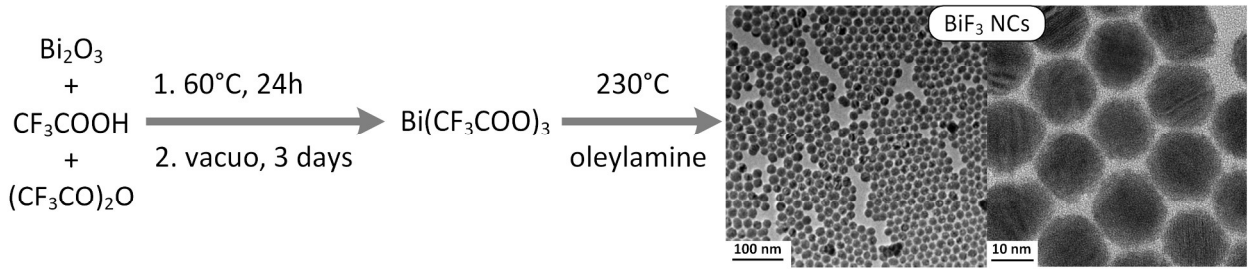


**Figure 1**. Schematic of the synthesis of $BiF_3$ NCs and transmission electron microscopy images of a ~15 nm sample. See ESI for synthesis details.

Our synthesis of $BiF_3$ NCs employed Bi(III) trifluoroacetate, $Bi(TFA)_3$, as a single-source precursor, using inexpensive starting reagents (Fig. 1). $Bi(TFA)_3$ was prepared as described by Reiss *et al.* (see ESI for details).[24] Elemental analysis of $Bi(TFA)_3$ provided a C:F ratio of 0.44 (theoretical: 0.4). The vacuum-dried precursor was then used in the synthesis of $BiF_3$ NCs. Stock precursor solution was prepared by dissolving $Bi(TFA)_3$ in distilled oleylamine. The thermal decomposition of TFA proceeds via decarboxylation, formation of the trifluoromethyl anion ($CF_3^-$) and its subsequent dissociation into a fluoride ion ($F^-$) and difluoromethylene ($CF_2$).[25] $F^-$ can then be combined with a metal ion to form the corresponding metal fluoride. As early as 1968,[26] trifluoroacetates $M(CF_3COO)_n$ of Cr(III), Fe(II), Co(II), Mn(II), Cu(II) and Zn(II) were reported to yield metal fluoride powders upon thermal decomposition at 200-300 °C. When decomposition is carried out in a suitable solvent and in the presence of surfactant molecules, the resulting fluorides can adopt the form of uniform colloidal NCs (Fig. 1). In our experiments, thermal decomposition was triggered by the injection of $Bi(TFA)_3$ precursor solution into hot (230 °C) oleylamine, yielding $BiF_3$ NCs in several minutes. Oleylamine served as both a high-boiling solvent and the surfactant. In similar recent work, monodisperse NCs of rare-earth metal fluorides (*e.g.,* $GdF_3$ and β-$NaYF_4$)[27, 28] and transition metal fluorides ($NaMF_3$, M=Mn, Co, Ni and Mg)[29] have been derived from corresponding TFA-complexes.

Detailed structural characterization of the NCs obtained in this work with high-resolution transmission electron microscopy (HRTEM, Fig. 2A), selected area electron diffraction (SAED, Fig. 2B) and powder X-ray diffraction (XRD, Fig. 2C) confirmed the formation of highly crystalline $BiF_3$. All of the SAED rings and XRD peaks match cubic $BiF_3$ (JCPDS entry no. 73-1988, space group Fm-3m, lattice constant a = 5.849 Å). Reactions conducted at temperatures higher than 250-260 °C typically yielded metallic Bi NPs due to the reduction of $Bi^{3+}$ by oleylamine. Reaction temperatures lower than ~180 °C are too low to induce the decomposition of $Bi(TFA)_3$, as confirmed by the combined thermogravimetrydifferential scanning calorimetry-mass spectrometry analysis (Fig. S1). The mean size of the $BiF_3$ NCs could be tuned from 6 to 50 nm by adjusting the concentrations of the precursors (Fig. S2, Table S1). Oleic acid was added during the purification stage to displace weakly bound oleylamine molecules and to maintain the colloidal stability of the $BiF_3$ NCs.

The electrochemical performance of the $BiF_3$ NCs was evaluated in custom-made Swagelok-type cells, constructed of titanium, with metallic Li as a counter and quasi-reference electrode.

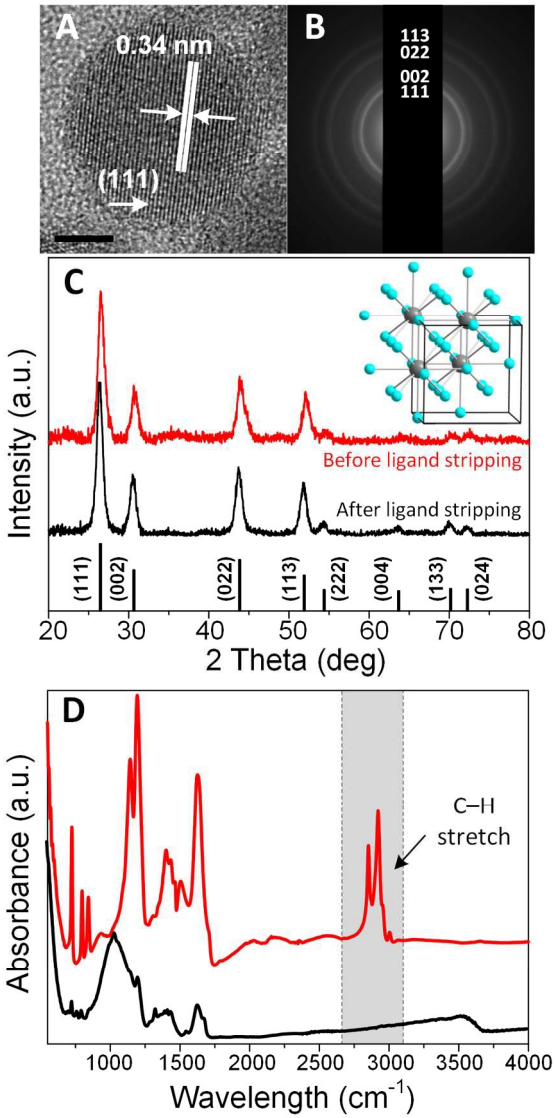


**Figure 2**. HRTEM image of a single $BiF_3$ NC (scale bar is 5 nm) (A), SAED of $BiF_3$ NCs from an area of ~1 $\mu m^2$ (B) and powder XRD patterns (C) and ATR-FTIR spectra (D) of $BiF_3$ NC samples before and after ligand stripping.

In construction of the electrochemical cells, good electronic connectivity between the NCs and current collectors must be established. As a first step, electrically insulating long-chain capping ligands (oleylamine/oleic acid) were removed with a 0.2 M solution of trimethyloxonium tetrafluoroborate in acetonitrile, as commonly used for other colloidal NC materials.[30, 31] A comparison of the intensities of aliphatic C–H stretching modes in the attenuated total reflectance Fourier-transform infrared spectra (ATR-FTIR, Fig. 2D) confirmed the complete removal of the organic capping layer. Other common ligand removal methods such as treatment with hydrazine or thermal annealing lead to the reduction of $BiF_3$ to $Bi^0$. As a second step, working electrodes containing 50 wt% of ~15 nm $BiF_3$ NCs, 40 wt% of carbon black as the conductive matrix and 10 wt% of polyvinylidene fluoride (PVDF) as a polymer binder were fabricated, with mass loading of 0.3 mg $cm^{-2}$. For this, all components were blended into homogeneous slurry by mixing with N-methyl-2-pyrrolidone (NMP) as a solvent. The electrode films were then obtained by casting the slurry onto Al foil, followed by vacuum drying at 80 °C for few days.

Discharge capacity and cycling stability of ~15nm $BiF_3$ NCs are presented in Fig. 3A. $BiF_3$ is characterized by a relatively high discharge/charge polarization of ca ~0.3 V and the amount of polarization varies with cycling in a similar manner to cycling stability. During the first 5 galvanostatic discharge/charge cycles the electrode maintained the theoretical capacity of the active material; however, the capacity quickly faded in subsequent cycles. Similar observations were reported for ball-milled $BiF_3$ nanocomposites by Amatucci *et al.*,[16, 20] confirming that this degradation upon extended cycling is a common challenge for $BiF_3$ cathodes. Metallic Bi, formed during discharge, may catalyse the reductive decomposition of the carbonates used as electrolyte solvents, even at potentials above 2 V.[19] Decomposition products form a solid-electrolyte interface (SEI) layer, which eventually insulates the individual NCs. The SEI layer itself may also undergo a partial decomposition during charging at higher voltages, as can be seen in voltage profiles and in cyclic voltammograms (Fig. 3C), where in addition to clear lithiation/delithiation features at 2.7-3.4 V, the anodic and cathodic reactions at < 2.3 V and > 3.6 V, respectively, can be seen. Furthermore, oxygen-rich decomposition products (e.g. $CO_2$, CO, carboxylic acid anhydrides, aldehydes, esters, ethylene oxide and oligomeric compounds) may result in the formation of $BiO_xF_{3-2x}$ and further destabilize the electrode material.[20, 32-35] Hence, for higher cycling stability, further work on the formulation of the electrodes (*e.g.,* carbon encapsulation) and the choice of electrolyte (*e.g.,* non-carbonate solvents) is required, while here we focus on the utility of $BiF_3$ NCs as a cathode material. The first discharge curve exhibits a rather low voltage of ~2.5 V, which may indicate a purely kinetic effect, as has also been observed by Amatucci *et al.*[17] In the second and third discharges, higher average voltages are observed, presumably due to favourable effects of restructuring during cycling. The following discharge curves are characterized by lower capacities and voltages (e.g., the $10^{th}$ cycle shown in Fig 3B). The decreasing voltage may be explained by the formation of the oxofluoride phase, due to reaction with oxygen-rich products of SEI decomposition.[36] These results clearly indicate that major improvements on the electrolyte are needed before applying $BiF_3$ as a cathode in Li-ion batteries. First promising results utilizing the LiTFSI+$LiBF_4$/adiponitrile system were recently reported.[37] The capacity retention was ~75% after 100 cycles, though at a very low C-rate (0.05).

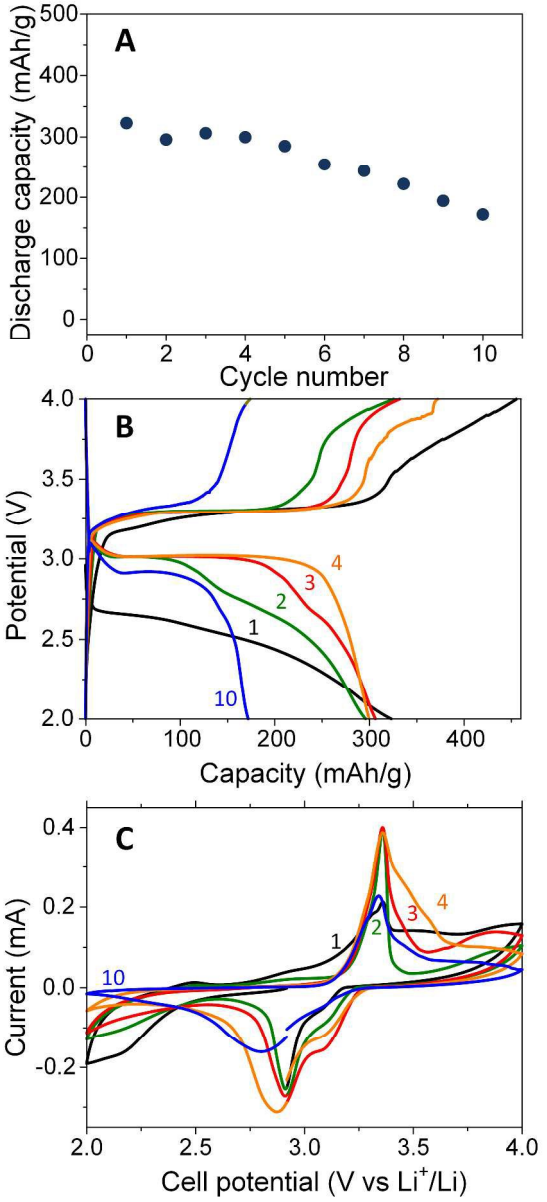


**Figure 3**. Electrochemical measurements of $BiF_3$ NCs: galvanostatic cycling stability at a current density of 50 mA $g^{-1}$ in the range of 2-4 V vs $Li/Li^+$ (A), galvanostatic discharge and charge curves (B) and cyclic voltammograms at a scan rate of 0.1 mV $s^{-1}$ (C).

In summary, we report a facile colloidal synthesis of $BiF_3$ NCs from an inexpensive precursor, with mean sizes tunable in the range of 6-50 nm. After stripping off the capping ligands, the $BiF_3$ NCs were tested as a cathode material for Li-ion batteries. The half-cell measurements showed that the theoretical specific Li capacity could be obtained. The cycling stability was comparable with other

reports, where nanostructuring of $BiF_3$ was obtained via top-down techniques. Further work is needed to stabilize the long-term operation of $BiF_3$ through advancement in the electrolyte chemistry.

## Acknowledgments

This work was financially supported by the Competence Center for Energy and Mobility (CCEM, Project SLIB), ETH Zürich (Grant Nr. ETH-56 12-2), Swiss Federal Commission for Technology and Innovation (CTI-Project Nr. 14698.2 PFIW-IW), CTI Swiss Competence Centers for Energy Research (SCCER Heat and Electricity Storage) and SNF Ambizione Energy grant (PZENP2_154287). Electron microscopy was performed at the Empa Electron Microscopy Center. We thank Dr. Christian Mensing for thermal analysis of $Bi(TFA)_3$ and Dr. Nicholas Stadie for reading the manuscript.

## Notes and references

[a] ETH Zürich – Swiss Federal Institute of Technology Zürich, Vladimir Prelog Weg 1, CH-8093 Zürich, Switzerland. E-mail: mvkovalenko@ethz.ch

[b] Empa-Swiss Federal Laboratories for Materials Science and Technology, Laboratory for Thin Films and Photovoltaics, Überlandstrasse 129, CH-8600 Dübendorf, Switzerland

† Electronic Supplementary Information (ESI) available: materials and methods, TG/DSC/MS of the $Bi(TFA)_3$ precursor, additional TEM images. See DOI: 10.1039/c000000x/

1. J.-M. Tarascon, *Phil. Trans. R. Soc. A*, 2010, **368**, 3227-3241.
2. L. Xu, C. Kim, A. K. Shukla, A. Dong, T. M. Mattox, D. J. Milliron and J. Cabana, *Nano Lett.*, 2013, **13**, 1800−1805.
3. K. Kravchyk, L. Protesescu, M. I. Bodnarchuk, F. Krumeich, M. Yarema, M. Walter, C. Guntlin and M. V. Kovalenko, *J. Am. Chem. Soc.*, 2013, **135**, 4199-4202.
4. M. I. Bodnarchuk, K. V. Kravchyk, F. Krumeich, S. Wang and M. V. Kovalenko, *ACS Nano*, 2014, **8**, 2360-2368.
5. M. He, K. V. Kravchyk, M. Walter and M. V. Kovalenko, *Nano Lett.*, 2014, **14**, 1255-1262.
6. B. Koo, H. Xiong, M. D. Slater, V. B. Prakapenka, M. Balasubramanian, P. Podsiadlo, C. S. Johnson, T. Rajh and E. V. Shevchenko, *Nano Lett.*, 2012, **12**, 2429−2435.
7. H. Wang, L.-F. Cui, Y. Yang, H. S. Casalongue, J. T. Robinson, Y. Liang, Y. Cui and H. Dai, *J. Am. Chem. Soc.*, 2010, **132**, 13978–13980.
8. X. Xu, R. Cao, S. Jeong and J. Cho, *Nano Lett.*, 2012, **12**, 4988−4991.
9. S. H. Lee, S.-H. Yu, J. E. Lee, A. Jin, D. J. Lee, N. Lee, H. Jo, K. Shin, T.-Y. Ahn, Y.-W. Kim, H. Choe, Y.-E. Sung and T. Hyeon, *Nano Lett.*, 2013, **13**, 4249−4256.
10. M. H. Oh, T. Yu, S.-H. Yu, B. Lim, K.-T. Ko, M.-G. Willinger, D.-H. Seo, B. H. Kim, M. G. Cho, J.-H. Park, K. Kang, Y.-E. Sung, N. Pinna and T. Hyeon, *Science*, 2013, **340**, 964-968.
11. M. He, M. Walter, K. V. Kravchyk, R. Erni, R. Widmer and M. V. Kovalenko, *Nanoscale*, 2015, **7**, 455-459.
12. M. F. Oszajca, M. I. Bodnarchuk and M. V. Kovalenko, *Chem. Mater.*, 2014, **26**, 5422−5432.
13. P. Gibot, M. Casas-Cabanas, L. Laffont, S. Levasseur, P. Carlach, S. Hamelet, J.-M. Tarascon and C. Masquelier, *Nat. Mater.*, 2008, **7**, 741-747.
14. S. Goriparti, E. Miele, F. De Angelis, E. Di Fabrizio, R. Proietti Zaccaria and C. Capiglia, *J. Power Sources*, 2014, **257**, 421-443.
15. N. Nitta, F. Wu, J. T. Lee and G. Yushin, *Mater.Today*, 2015, **18**, 252-264.
16. J. Cabana, L. Monconduit, D. Larcher and M. R. Palacín, *Adv. Mater.*, 2010, **22**, E170-E192.
17. M. Bervas, F. Badway, L. C. Klein and G. G. Amatucci, *Electrochem. Solid State Lett.*, 2005, **8**, A179-A183.
18. M. Bervas, A. N. Mansour, W.-S. Yoon, J. F. Al-Sharab, F. Badway, F. Cosandey, L. C. Klein and G. G. Amatucci, *J. Electrochem. Soc.*, 2006, **153**, A799-A808.
19. A. J. Gmitter, F. Badway, S. Rangan, R. A. Bartynski, A. Halajko, N. Pereira and G. G. Amatucci, *J. Mater. Chem.*, 2010, **20**, 4149–4161.
20. A. J. Gmitter, A. Halajko, P. J. Sideris, S. G. Greenbaum and G. G. Amatucci, *Electrochim. Acta*, 2013, **88**, 735-744.
21. B. Hu, X. Wang, H. Shu, X. Yang, L. Liu, Y. Song, Q. Wei, H. Hu, H. Wu, L. Jiang and X. Liu, *Electrochim. Acta*, 2013, **102**, 8-18.
22. B. Hu, X. Wang, Y. Wang, Q. Wei, Y. Song, H. Shu and X. Yang, *J. Power Sources*, 2012, **218**, 204-211.
23. J. Zhao, H. Pan, X. He, Y. Wang, L. Gu, Y.-S. Hu, L. Chen, H. Liu and S. Dai, *Nanoscale*, 2013, **5**, 518-522.
24. G. J. Reiss, W. Frank and J. Schneider, *Main Group Met. Chem.*, 1995, **18**, 287-294.
25. P. G. Blake and H. Pritchard, *J. Chem. Soc. B*, 1967, 282-286.
26. M. J. Baillie, D. H. Brown, K. C. Moss and D. W. A. Sharp, *J. Chem. Soc. A.*, 1968, 3110-3114.
27. X. Ye, J. E. Collins, Y. Kang, J. Chen, D. T. N. Chen, A. G. Yodh and C. B. Murray, *Proc. Natl. Acad. Sci. U.S.A.*, 2010, **107**, 22430-22435.
28. T. Paik, D.-K. Ko, T. R. Gordon, V. Doan-Nguyen and C. B. Murray, *ACS Nano*, 2011, **5**, 8322-8330.
29. Y. P. Du, Y. W. Zhang, Z. G. Yan, L. D. Sun, S. Gao and C. H. Yan, *Chem.-Asian J.*, 2007, **2**, 965-974.
30. E. L. Rosen, R. Buonsanti, A. Llordes, A. M. Sawvel, D. J. Milliron and B. A. Helms, *Angew. Chem. Int. Ed.*, 2012, **51**, 684-689.
31. R. Buonsanti, T. E. Pick, N. Krins, T. J. Richardson, B. A. Helms and D. J. Milliron, *Nano Lett.*, 2012, **12**, 3872−3877.
32. M. Arakawa and J.-i. Yamaki, *J. Power Sources*, 1995, **54**, 250-254.
33. M. Moshkovich, M. Cojocaru, H. E. Gottlieb and D. Aurbach, *J. Electroanal. Chem.*, 2001, **497**, 84-96.
34. K. Kanamura, S. Toriyama, S. Shiraishi, M. Ohashi and Z.-i. Takehara, *J. Electroanal. Chem.*, 1996, **419**, 77-84.
35. L. Xing, W. Li, C. Wang, F. Gu, M. Xu, C. Tan and J. Yi, *J. Phys. Chem. B*, 2009, **113**, 16596–16602.
36. M. Bervas, L. C. Klein and G. G. Amatucci, *J. Electrochem. Soc.*, 2006, **153**, A159-A170.
37. A. J. Gmitter, J. Gural and G. G. Amatucci, *J. Power Sources*, 2012, **217**, 21-28.



 

TOC graphics: